Formation of large-grain-sized $BaSi_2$ epitaxial layers grown on Si(111) by molecular beam epitaxy

M. Baba[a], K. Toh[a], K. Toko[a], K. O. Hara[b], N. Usami[b,d], N. Saito[c], N. Yoshizawa[c], and T. Suemasu[a,d]

[a]*Institute of Applied Physics, University of Tsukuba, Tsukuba, Ibaraki 305-8573, Japan*

[b]*Institute for Materials Research,University of Tohoku, Sendai, Miyagi 980-8577, Japan*

[c]*Electron Microscope Facility, IBEC Innovation Platform, AIST, Tsukuba 305-8569*

[d]*Japan Science and Technology Agency, CREST, Chiyoda, Tokyo 102-0075, Japan*

Corresponding author: T. Suemasu

Institute of Applied Physics, University of Tsukuba, Tsukuba, Ibaraki 305-8573, Japan

TEL/FAX: +81-29-853-5111, Email: suemasu@bk.tsukuba.ac.jp

$BaSi_2$ epitaxial films were grown on Si(111) substrates by a two-step growth method including reactive deposition epitaxy (RDE) and molecular beam epitaxy (MBE). To enlarge the grain size of $BaSi_2$, the Ba deposition rate and duration were varied from 0.25 to 1.0 nm/min and from 5 to 120 min during RDE, respectively. The effect of post-annealing was also investigated at 760 °C for 10 min. Plan-view transmission electron micrographs indicated that the grain size in the MBE-grown $BaSi_2$ was significantly increased up to approximately 4.0 μm, which is much larger than 0.2 μm, reported previously.

PACS: 78.40.Fy

Keywords: B1. Semiconducting silicides; B2. $BaSi_2$; B3. Solar cell; A3. MBE; A1. Large grain

1. Introduction

The solar cell market has been growing rapidly with the increasing demand for renewable energy, and new materials for high-efficiency thin-film solar cells are of significant interest. However, little steadfast effort has been devoted to any materials other than Si, CIGS (copper indium gallium selenide), CdTe and III-V compounds as far as inorganic semiconductors are concerned. Among such materials, we have focused on barium disilicide ($BaSi_2$) as a promising material for solar cell applications. Semiconducting $BaSi_2$ has a band gap of approximately 1.3 eV and a very large absorption coefficient of 3×10^4 cm^{-1} at 1.5 eV [1-3]. In our previous works, we have achieved large photoresponsivities in undoped *n*-type $BaSi_2$ epitaxial layers on Si(111) and polycrystalline $BaSi_2$ layers on SiO_2 [4-6]. $BaSi_2$ can be grown epitaxially on both Si(111) and Si(001) [7,8]. Very recently, we have found a large minority-carrier diffusion length of over 9 μm in undoped *n*-type $BaSi_2$ epitaxial layers [9]. Thus, $BaSi_2$ is considered to be a promising material for solar cell applications. However, the grain size of $BaSi_2$ epitaxial films is typically as small as approximately 0.2 μm [9], due to three epitaxial variants rotated by 120° about the surface normal [10]. Grain boundaries (GBs) often function as recombination centers for minority carriers [11,12]; therefore, improved photoresponsivity in $BaSi_2$ epitaxial films is expected with much larger grains. Thus, the formation of large grains is important for solar cell applications. We have previously succeeded in the expansion of $BaSi_2$ grains in films using vicinal Si(001) and Si(111) substrates [13,14]. In this paper, we aimed to form large-grain-sized $BaSi_2$ exceeding 1 μm on exact Si(111) substrates by adjusting the growth conditions and post-annealing.

2. Experimental

A two-step growth method was adopted that included reactive deposition epitaxy (RDE; Ba deposition on hot Si) for $BaSi_2$ template layers [15], and subsequent molecular beam epitaxy (MBE; codeposition of Ba and Si on Si) to form thick $BaSi_2$ films. Details of the growth procedure have been previously described [9,13]. Prior to growth, exact Si(111) substrates were cleaned by RCA washing, followed by thermal cleaning in ultrahigh vacuum. A 7×7 streaky reflection high-energy electron diffraction (RHEED) pattern indicated that a clean Si surface was obtained. The sample preparation details are summarized in Table 1. The substrate temperature T_{RDE}, was set to 500 or 600 °C, and the Ba deposition rate R_{Ba}, was varied from 0.25 to 1.0 nm/min to form $BaSi_2$ template layers by RDE. Also the duration of growth by RDE t_{RDE}, was increased from 5 to 120 min, while R_{Ba} was decreased from 1 to 0.25 nm/min to enhance migration of Ba atoms on the surface. t_{RDE} was determined so that the entire Si surface was covered sufficiently with $BaSi_2$ template layers by atomic force microscopy (AFM). Both Ba and Si were then deposited on these template layers to form $BaSi_2$ by MBE. The substrate temperature T_{MBE} was set to 580 °C, and the MBE growth duration t_{MBE} was 60 min for 100-nm-thick $BaSi_2$ in samples A-D, and 240 min for

500-nm-thick $BaSi_2$ in sample E. Post annealing was performed for samples D and E at 760 °C for 10 min after MBE. This temperature was chosen because the desorption of Ba atoms from grown $BaSi_2$ films occurs around 800 °C. The crystalline quality of the films was evaluated using RHEED, θ-2θ X-ray diffraction (XRD) and the crystal-plane direction was observed using electron backscatter diffraction (EBSD). The EBSD measurement was carried out at intervals of 0.1 μm. Transmission electron microscopy (TEM; Topcon EM-002B, operated at 120 kV) of film surfaces after mechanical polishing and ion milling was employed to investigate the grain size of $BaSi_2$.

3. Results and discussion

Sharp streaky RHEED patterns were obtained for samples A-D, observed along the Si[1-10] azimuth, and θ-2θ XRD peaks of only (100)-oriented $BaSi_2$ planes, such as the (200), (400) and (600) planes were obtained, as previously reported [9]. These results indicate the successful growth of highly *a*-axis-oriented $BaSi_2$ epitaxial films.

Figures 1(a)-1(c) show the AFM images taken after RDE growth for samples A-C, respectively. Many island domains of approximately 0.3 μm in size are evident in Fig. 1(a). As R_{Ba} is decreased, and both t_{RDE} and T_{RDE} are increased, step-and-terrace structures become dominant, as shown in Figs. 1(b) and 1(c). The step height is approximately 0.9 nm, which corresponds to *a*-axis lattice parameter in $BaSi_2$ [16,17]. This is attributed to enhanced lateral migration of Ba atoms on the surface.

Figures 2(a)-2(d) show dark-field (DF) plan-view TEM observations for samples A-D, taken under a two-beam diffraction condition to clarify the grain size of $BaSi_2$. Selected-area diffraction (SAED) patterns are also shown. The diffraction vector g was set to be <004>. Under these conditions, the diffraction spot corresponding to the (004) plane becomes bright in the SAED patterns, while other spots denoted by (00n) (n=$\pm 1, \pm 2, \pm 3, \ldots$) are also evident. Note that those $BaSi_2$ grains that satisfy Bragg's condition of diffraction become bright; one of the three $BaSi_2$ epitaxial variants becomes bright, which provides information regarding the grain size. A detailed discussion of the grain boundaries (GBs) in $BaSi_2$ was given in our previous report [9]. Figure 2(a) shows that the grain size of $BaSi_2$ is approximately 0.2 μm in sample A, which is typical for $BaSi_2$ layers [9]. The grains in samples B and C are significantly expanded, showing that the grains of the RDE-grown $BaSi_2$ template layers significantly affect those of MBE-grown $BaSi_2$ films. Regarding sample D, the curvature of the sample made it difficult to investigate the grain size of $BaSi_2$ by TEM, but the grain size in sample D became apparently larger than that in sample A. This means that the post-annealing is a very effective means to enhance the grain size of $BaSi_2$. The difference in growth conditions between samples A and D is that the post-annealing was performed on sample D. Thus, it is considered that the 0.2-μm-sized $BaSi_2$ grains in sample A coalesced with each other during the post-annealing, growing in much larger grains.

In order to observe the $BaSi_2$ grains in the wider range, EBSD mappings were performed. Figures 3(a)-3(d) show EBSD images obtained along the transverse direction (TD) for samples A-C and E, respectively. We can see three colors represented by red, green, and blue, indicating three epitaxial variants of *a*-axis-oriented $BaSi_2$ on Si(111) [9,10]. The grain size can be roughly determined from the areas of regions with the same color. As shown in Fig. 3 (b), the grains in sample B are the largest among the four, extending to more than 4 μm, and this is the largest grain we have ever achieved. In Fig. 3(b), green area dominates. But we don’t think that there is a mechanism which makes one of the three domains larger than the others. Observation of EBSD mappings in a much wider area will give us correct EBSD mappings. The grain size of $BaSi_2$ in sample C is approximately 2.0 μm, which is also much larger than that in sample A, but smaller than that in sample B, indicating that there is an optimum condition for RDE to expand the grains of $BaSi_2$. As for the effect of post-annealing, the grains in sample E are much larger than that in sample A. As discussed in Fig. 2(d), post-annealing also increased the grains of 100-nm-thick $BaSi_2$ in sample D. On the basis of these results, we concluded that the optimization of RDE growth conditions for large-grained $BaSi_2$ templates and the post-annealing are both effective to enlarge the grains of $BaSi_2$ epitaxial films on Si(111).

4. Summary

We attempted to grow $BaSi_2$ epitaxial layers with large grains by adjusting the RDE growth conditions and the post-annealing, and successfully achieved a grain size of over 4.0 μm by decreasing R_{Ba} and increasing t_{RDE}. The grain size was confirmed by plan-view TEM observations and EBSD maps. We also found that post-annealing at 760 °C for 10 min extended the grains of $BaSi_2$.

Acknowledgements

This work was financially supported by the Japan Science and Technology Agency (JST/CREST). TEM observations were conducted at the Electron Microscope Facility supported by the IBEC Innovation Platform of AIST, Japan. EBSD observations were conducted at Institute for Materials Research of Tohoku University.

References

[1] K. Morita, Y. Inomata, T. Suemasu, Thin Solid Films 508 (2006) 363.

[2] D. B. Migas, V. L. Shaposhnikov, V.E. Borisenko, Phys. Status Solidi B 244 (2007) 2611.

[3] K. Toh, T. Saito, T. Suemasu, Jpn. J. Appl. Phys. 50 (2011) 068001.

[4] W. Du, M. Suzuno, M. A Khan, K. Toh, M. Baba, K. Nakamura, K. Toko, N. Usami, T. Suemasu, Appl. Phys. Lett. 100 (2012) 152114.

[5] Y. Matsumoto, D. Tsukada, R. Sasaki, M. Takeishi, T. Suemasu, Appl. Phys. Express 2 (2009) 021101.

[6] D. Tsukada, Y. Matsumoto, R. Sasaki, M. Takeishi, T. Saito, N. Usami, T. Suemasu, Appl. Phys. Express 2 (2009) 051601.

[7] R. A. Mckee, F. J. Walker, J. R. Conner, E. D. Specht, D. E. Zelmon, Appl. Phys. Lett. 59 (1991) 782.

[8] R. A. Mckee, F. J. Walker, Appl. Phys. Lett. 63 (1993) 2818.

[9] M. Baba, K. Toh, K. Toko, N. Saito, N. Yoshizawa, K. Jiptner, T. Sekiguchi, K. O Hara, N. Usami, T. Suemasu, J. Cryst. Growth 348 (2012) 75.

[10] Y. Inomata, T. Nakamura, T. Suemasu, F. Hasegawa, Jpn. J. Appl. Phys. 43 (2004) L478.

[11] J. Chen, T. Sekiguchi, D. Yang, F. Yin, K. Kido, S. Tsurekawa, J. Appl. Phys. 96 (2004) 5490.

[12] I. Gordon, L. Carnel, D. Van Gestel, G. Beaucarne, J. Poortmans, Thin Solid Films 516

(2008) 6984.

[13] K. Toh, K. O. Hara, N. Usami, N. Saito, N. Yoshizawa, K. Toko, T. Suemasu, J. Cryst. Growth 345 (2012) 16.

[14] K. O. Hara, N. Usami, K. Toh, K. Toko, T. Suemasu, Jpn. J. Appl. Phys. 51 (2012) 10NB06.

[15] Y. Inomata, T. Nakamura, T. Suemasu, F. Hasegawa, Jpn. J. Appl. Phys. 43 (2004) 4155.

[16] J. Evers, G. Oehlinger, A. Weiss, Angew. Chem., Int. Ed. 16 (1977) 659.

[17] M. Imai, T. Hirano, Phys. Rev. B 58 (1998) 11922.

Fig. 1. (a)-(c) AFM images after RDE growth for samples A-C, respectively.

Fig. 2. DF TEM images for (a) sample A, (b) sample B, (c) sample C, and (d) sample D obtained under a two-beam diffraction condition using the diffraction vector g = <004> for one of the three epitaxial variants.

Fig. 3. TD EBSD images for (a) sample A, (b) sample B, (c) sample C, and (d) sample E. The relationship between the three epitaxial variants (red, green, and blue) are also shown.

Table 1: Growth conditions for samples A-E.

Sample	R_{Ba} (nm/min)	T_{RDE} (°C)	t_{RDE} (min)	T_{MBE} (°C)	t_{MBE} (min)	Annealing
A	1.0	500	5	580	60	w/o
B	0.5	600	60	580	60	w/o
C	0.25	600	120	580	60	w/o
D	1.0	500	5	580	60	760 °C, 10 min
E	1.0	500	5	580	240	760 °C, 10 min

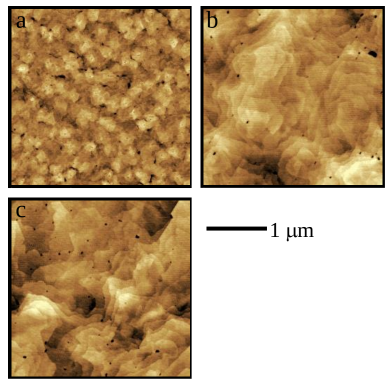

Fig. 1

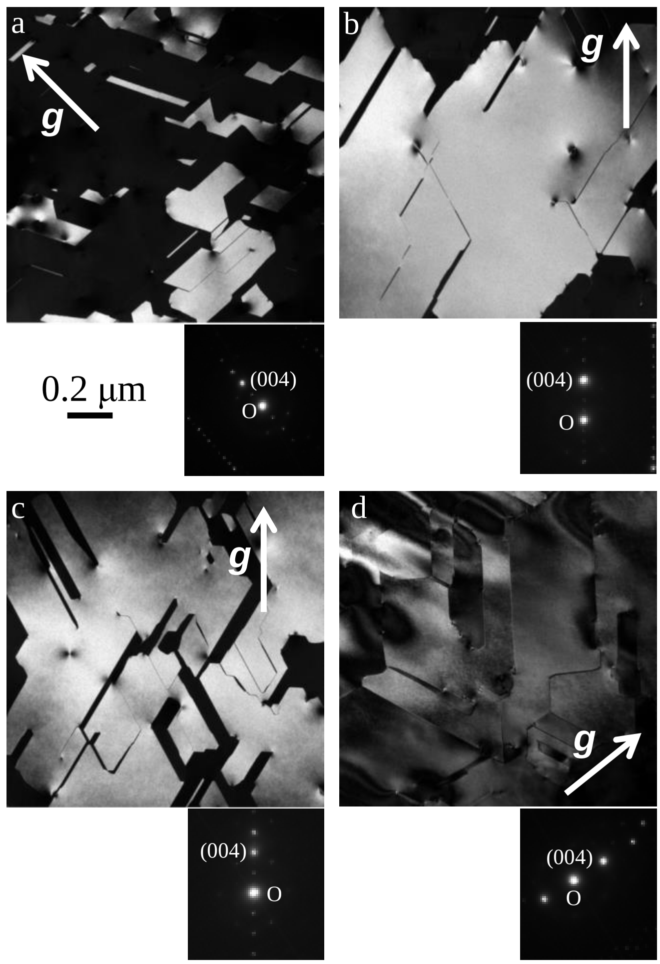

Fig. 2

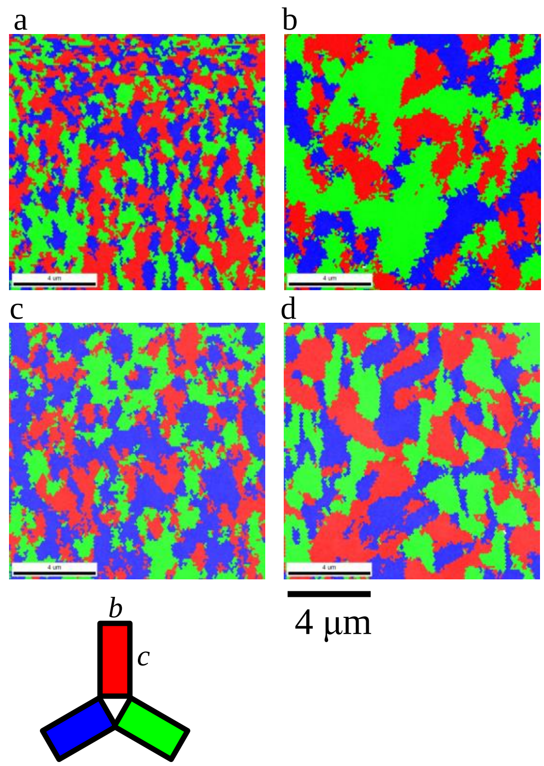

Fig. 3